

Space-Charge Measurement Technologies and Their Potential Applications

Rongsheng Liu,^{*} Christer Törnkvist, and Marc Jeroense¹

ABB AB, Corporate Research, 721 78 Västerås, Sweden

¹NKT HV Cables AB, 371 23 Karlskrona, Sweden

(Received November 25, 2016; accepted March 22, 2017)

Keywords: space charge, insulation, measurement methods, sensors, power devices

The development history of major space-charge measurement technologies is reviewed. Advantages and disadvantages are analyzed regarding the electron beam, thermal pulse, pressure wave, pulsed electroacoustic wave, electrooptic Kerr effect, and Pockels effect methods. Measurement technologies are discussed further with regard to principles, know-how, and milestones of development. With the pulsed electroacoustic method as an example, a deconvolution technique is introduced, as it is needed to quantify the density of space charge in a material. Potential applications of these technologies to measure the distribution of space charge in dielectrics and electrical insulation materials and systems are addressed. By the electrooptic Pockels effect method, two-dimensional discharge patterns on the surfaces of cellulose Kraft paper and Nomex T410 paper were measured and reported for the first time. With the progress of the technologies, it appears that today, sensors can be made to measure quantitatively the distribution of space charge in dielectrics and electrical insulation systems.

1. Introduction

Over the last 40 years, methods utilizing pressure pulses,^(1–14) electron beams,^(15–17) and thermal pulses^(18–20) have been developed for the measurement of space charge in solid insulating materials. The pressure pulse techniques have also been used for the measurement of space charge in composite oil/cellulose insulating systems.^(21–25) For the measurement of electric fields and space charge in liquid dielectrics and surface charge on solids in air, the electrooptic Kerr effect technique^(26–30) and Pockels effect technique^(31–33) have been developed. In comparison with the earliest slice method,⁽³⁴⁾ these latest techniques can be used to measure quantitatively the distribution of space charge in an insulating material nondestructively, and thus are valuable tools in helping to understand the electrical behaviors of an insulation system in the development of power equipment, such as high-voltage direct-current (HVDC) cables (Fig. 1) and converter transformers (Fig. 2).

^{*}Corresponding author: e-mail: rongsheng.liu@se.abb.com
<http://dx.doi.org/10.18494/SAM.2017.1506>



Fig. 1. (Color online) Extruded cross-linked polyethylene (XLPE) DC cable at ± 640 kV.



Fig. 2. (Color online) Converter transformer at ± 1100 kV.

2. Principles of Space Charge Measurement Techniques

The electron beam method was proposed in the late 1970s.⁽¹⁵⁾ An electron beam is used as a source of excitation. A solid sample is irradiated by the electron beam with stepped energy levels. The electric conductivity of the sample increases in the irradiated region of the material, and the space charge within the region is compensated. The electron beam functions as a virtual probe. Under a short-circuit condition or with a biased DC voltage, induction charges on the back electrode were released with each step increase in the electron beam energy. With the electron beam penetrating through the entire thickness of the sample, the distribution of space charge in the sample was measured using

$$\rho(s) = -\frac{d^2(qs)}{ds^2}. \quad (1)$$

Here, s is the thickness of the nonirradiated region, q is the induced charge density on the back electrode, and $\rho(s)$ is the space charge density inside the sample.

The electron beam method is a destructive method; however, it has the advantage of high resolution. The spatial resolution of the space charge distribution can be as fine as $1 \mu\text{m}$, and thus is especially suitable for thin samples.

The thermal pulse method was proposed in the middle of the 1970s.⁽¹⁸⁾ The principle of the method is as follows. A metallized sample is irradiated, for example, by a light pulse. The light pulse is absorbed by the sample surface and converted into thermal energy, which diffuses into the body of the sample. A temperature distribution across the sample is created and it varies with time. The thickness and permittivity of the sample vary as well. The surface potential on the metallized sample electrode varies with time. The distribution of space charge in the sample is then obtained through a deconvolution of

$$\Delta V(t) = \frac{(\alpha_x - \alpha_\varepsilon)}{\varepsilon_0 \varepsilon} \int_0^d \left[\rho(x) \int_0^x \Delta T(x', t) dx' \right] dx. \quad (2)$$

Here, ε_0 is the dielectric constant of free space, and α_x , α_ε , and ε are the thermal expansion coefficient, thermal coefficient of permittivity, and relative permittivity of the sample, respectively. d is the thickness of the sample, V is the surface potential of the electrode, $\Delta V(t)$ is the variation of V , and $\rho(x)$ and $\Delta T(x, t)$ are the space charge density and temperature rise at location x , respectively.

In comparison with the electron beam method, the thermal pulse method can use a light pulse that creates a limited temperature rise (such as less than 5 °C) in the sample, and thus, the latter is a nondestructive method. However, the method is complicated since a deconvolution technique is needed.

The pressure wave method was proposed in the late 1970s.⁽⁷⁾ A pressure wave can be produced with the use of a laser, a shock tube or a piezo device. With the pressure wave propagating through a sample, a nonuniform deformation of a local material, small displacement of space charge, and variation of permittivity occur. The voltage $V(t)$ and current $I(t)$ measurements on the sample are related to internal field in the following manner.

Under an open-circuit condition:

$$V(t) = \chi G(\varepsilon) \int_0^d E(z, 0) p(z, t) dz. \quad (3)$$

Under a short-circuit condition:

$$I(t) = \chi G(\varepsilon) C \int_0^d E(z, 0) \frac{\partial p(z, t)}{\partial t} dz. \quad (4)$$

Here, χ is the compressibility of the sample, $G(\varepsilon)$ is a function of the relative permittivity ε containing the dependence of ε on pressure, d is the thickness of the sample, C is the capacitance of the sample, $E(z, 0)$ is the electric field before the pressure wave propagation, and $p(z, t)$ is the profile of the pressure wave. The electric field and space charge distribution in the sample were obtained through a mathematical solution [either Eq. (3) or (4)]. The pressure pulse method has been widely used in the measurement of space charge in dielectric materials. However, for an advanced application, a deconvolution technique is required to obtain the space charge density while considering the attenuation and dispersion of the pressure wave propagation in the sample.

The pulsed electroacoustic (PEA) method was proposed in the early 1980s.⁽¹⁾ A pulsed voltage is applied to a sample. Space charges vibrate following the pulsed voltage in the sample, because Maxwell electromagnetic forces. Acoustic pulses are generated, propagated, and detected by a piezoelectric transducer. The transducer converts the acoustic pulses into a voltage signal, from which the distribution of space charge is obtained through deconvolution processing⁽⁶⁾ [Eqs. (5) through (8)].

$$\begin{aligned}
P(t) = & \frac{Z_1}{(Z_1 + Z_2)} \left\{ \left[\varepsilon_0 \varepsilon E(0) e \left(t - \frac{l}{u_1} \right) - \frac{1}{2} \varepsilon_0 \varepsilon e^2 \left(t - \frac{l}{u_1} \right) \right] \right. \\
& + \int_0^{u_2} \left(t - \frac{l}{u_1} \right) \rho(\xi) e \left(t - \frac{l}{u_1} - \frac{\xi}{u_2} \right) d\xi \\
& \left. + \frac{2Z_2}{Z_2 + Z_3} \left[-\varepsilon_0 \varepsilon E(d) e \left(t - \frac{l}{u_1} - \frac{d}{u_2} \right) + \frac{1}{2} \varepsilon_0 \varepsilon e^2 \left(t - \frac{l}{u_1} - \frac{d}{u_2} \right) \right] \right\} \quad (5)
\end{aligned}$$

$$v_s(t) = \int_{-\infty}^{\infty} P(\theta) h(t - \theta) d\theta \quad (6)$$

Here, ζ represents the variable of distance, θ denotes time, $P(t)$ is the generated pressure wave pulse, $\rho(\zeta)$ and $E(\zeta)$ are the space charge density and electric field in the sample, ε and d are the relative permittivity and thickness of the sample, l is the length of the ground electrode, Z_1 , Z_2 , and Z_3 are the acoustic impedances of the ground electrode, sample, and HV electrode, u_1 and u_2 are the acoustic velocities of the ground electrode and sample, and $h(t)$ and $v_s(t)$ are the response function of the delta function $\delta(t)$ and the output signal voltage of the piezo transducer, respectively. Equation (6) is the convolution equation. In a frequency domain, the Fourier transform of Eq. (6) is

$$V_{sF}(\omega) = P_F(\omega) H(\omega), \quad (7)$$

where $V_{sF}(\omega)$ and $P_F(\omega)$ are the Fourier transforms of $v_s(t)$ and $P(t)$, and $H(\omega)$ is the transfer function of the piezo transducer. With an inverse Fourier transform $F^{-1}[\]$, the pressure wave $P(t)$ is represented as

$$P(t) = F^{-1} [P_F(\omega)] = F^{-1} \left[\frac{V_{sF}(\omega)}{H(\omega)} \right]. \quad (8)$$

$V_{sF}(\omega)$ is a measurement result containing the distribution of space charge, $H(\omega)$ can be obtained from a calibration process before the sample is charged, where the calibration output signal voltage is obtained with the application of the so-called ‘‘calibration DC voltage’’ to the sample. The calibration DC voltage is so small that there is no space charge generated in the sample, and thus, the calibration output signal voltage contains only voltage peaks from the interfacial charges at the interfaces between the sample and the electrodes (to ensure that the sample is free of a volume space charge distribution in the application of the calibration DC voltage). $P(t)$ is obtained from Eq. (8). The distribution of space charge in the sample is then obtained through the Fourier transform of Eq. (5) and a further process of inverse Fourier transform.

At its beginning stage, the PEA method involved the use of a lead zirconate titanate (PZT) transducer, which has a limited bandwidth of frequency (such as with a bandwidth of 1 MHz at the central frequency of 10 MHz). A consequence was that the output signal voltage had a large oscillation. The measurement frequency bandwidth of the PEA method was significantly increased following the replacement of the PZT transducers by polyvinylidene fluoride (PVDF) transducers,^(6,35) and it became possible to measure space charge distributions sufficiently accurately without resorting to deconvolution procedures.

Electrooptic methods are based on electrooptic effects. Depending on the dielectric materials, the electrooptic effect may manifest as a linear electrooptic effect called the Pockels effect or as a quadratic electrooptic effect called the Kerr effect.⁽³⁶⁾ The difference in the two orthogonal refractive indices Δn ($= n_x - n_y$) is expressed using a power series with respect to an applied electric field as

$$\Delta n \cong \Delta n_0 + \Delta a E + \Delta b E^2. \quad (9)$$

Here, Δn_0 is the electric-field-independent natural birefringence, and Δa and Δb are the coefficients for the Pockels effect and Kerr effect, respectively. These two effects do not occur simultaneously, and only one effect occurs for any one material. Natural birefringence Δn_0 usually exists in solid materials. Because it changes with temperature, the natural birefringence is not desired for practical applications.

On the basis of the Kerr effect, measurement techniques were developed in the 1990s for the measurement of two-dimensional electric fields in dielectric liquids.^(26,29) At about the same period of time, measurement techniques were developed for the measurement of two-dimensional electric fields on the surface of dielectric solids in air using the Pockels effect.^(31–33)

3. Application Examples of Space Charge Measurement Techniques

The electron-beam and thermal-pulse techniques are suitable for the measurement of space charge distribution in a thin sample of solid dielectrics, for instance, with thickness in the order of microns. These techniques play an important role in the development of dielectrics, such as electrets.^(15–20) The pressure wave methods, pulsed electroacoustic methods, and electrooptic methods have more applications with solid and liquid dielectrics, such as in electrical insulation materials and the designs of electrical insulation systems. Applications regarding dielectrics and electrical insulation materials and systems are exemplified as follows.

3.1 Applications to electrical cables

A pressure wave propagation (PWP) method was introduced to measure the distribution of space charge in synthetic cables as early as 1989,^(37–39) where the space charge distribution was measured in a piece of low-density polyethylene (LDPE) cable with 5.5-mm-thick insulation. At about the same period of time, the PEA method was applied in measuring the space charge distributions in extruded cables under both DC and AC voltages^(40–43) (Fig. 3). For the PEA method, deconvolution was introduced for signal calibration in a cylindrical cable geometry,⁽⁴⁴⁾ and a flat electrode system was used for the measurement of space charge in the insulation of coaxial cables with insulation thickness up to the order of 20 mm.^(45–48) The method was also used to study the aging of an extruded cable under DC voltage application for up to 3 years.^(49,50)

With the development of the techniques and the needs of industry, the pressure wave methods, especially the pulsed electroacoustic method, have been presented in a Conseil International des Grands Réseaux Électriques (CIGRE) task force report and converted into an International Electrotechnical Commission (IEC) standard.^(13,14,51)

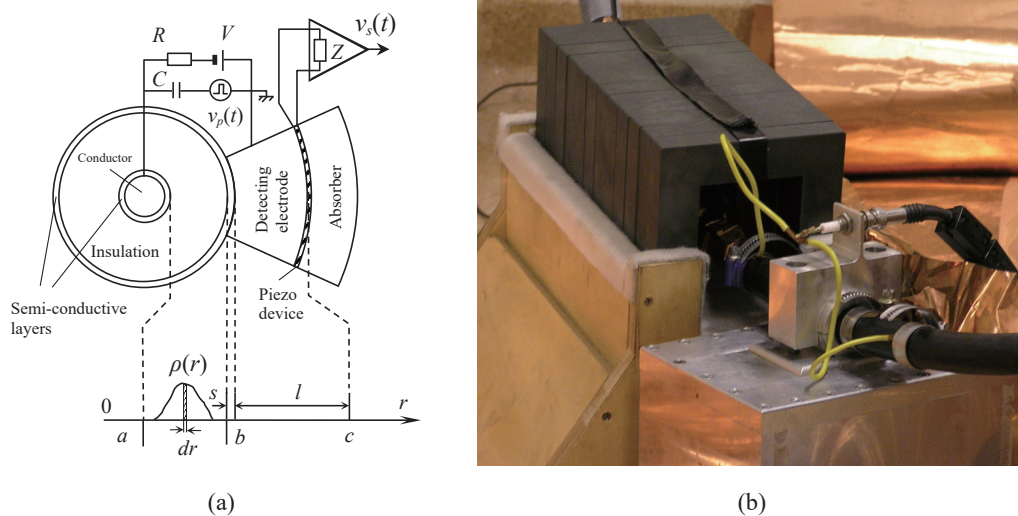


Fig. 3. (Color online) Application of the PEA method for the measurement of space charge in cylindrical cable geometry: (a) principle and (b) a measurement system. a and b are the inner and outer radii of the insulation, $\rho(r)$ is the volume space charge density at radius r , and s , l , and c are the thickness of the outer semiconductive layer, the distance between the outer semiconductive layer and the piezo device (a PVDF film), and the position of the piezo device, respectively. R and C are the resistance and capacitance of the PEA measurement system, respectively, V is the voltage of the DC source, and $v_p(t)$ is the time-dependent voltage output of the pulse generator. $v_s(t)$ is the output voltage from the piezo device, from which the space charge distribution is deduced.⁽⁴³⁾

In 1997, the PEA method was, for the first time, used to measure the distribution of space charge in the insulation materials of mass-impregnated nondraining (MIND) HVDC cables.⁽²⁵⁾

In the development of insulation materials for extruded cables, a package-charge-peak moving phenomenon was observed in 1988^(6,35,52) by the PEA method, where dc voltages of ± 70.7 kV were separately applied to polyethylene samples of 1 mm thickness, and a package charge peak was seen to move from one electrode to the other. This phenomenon was reported further at higher electric fields in the range of 100–400 kV/mm, which is close to the breakdown strength of LDPE.⁽⁵³⁾ Nowadays, the PEA method has been recognized as one of the most advanced methods for measuring the distribution of space charge in extruded cables.

3.2 Applications to power transformers

The PWP method has been used to measure the distribution of space charge in a composite oil-impregnated cellulose pressboard insulation system applied to converter transformers since 1992.^(21–24) We measured, for the first time, the distribution of space charge inside the pressboard as well as at the interface between a plain oil gap and a pressboard (Fig. 4). Measurement results were matched with the results of model simulation (Fig. 5), creating a bridge between the space charge measurement techniques and the design of power equipment, in this case, the design of an insulation system for an HVDC converter transformer.

However, it should be addressed that there was an issue in the PWP method with a laser being used as the source of pulsed radiation. The stability of the generated pressure pulses was

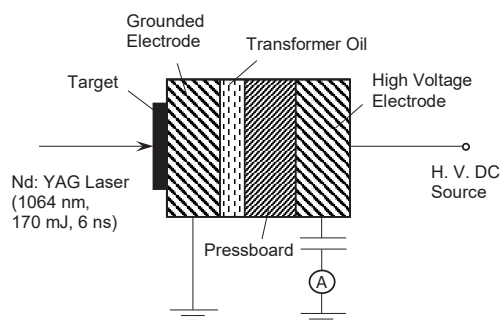


Fig. 4. PWP measurement system for the measurement of space charge in composite oil/pressboard insulation.

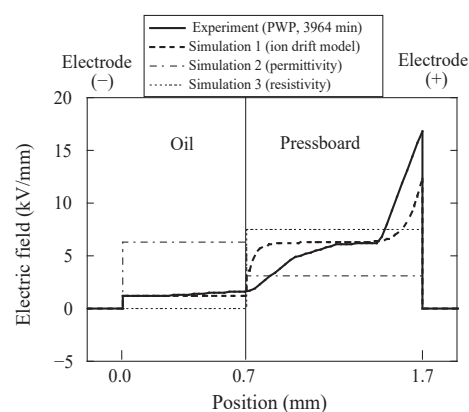


Fig. 5. Measurement and simulation results of electric fields in composite oil/pressboard insulation.

dependent on the target material and quality as well as the radiation energy level of the laser. Good measurement results were ensured when the generated pressure pulses were stabilized. There are alternative ways to produce the pressure pulses, such as by using a piezo device.^(13,14)

3.3 Applications of optic methods to insulation system for power equipment

A combination of optic methods and the PWP/PEA methods make it possible to measure the distribution of space charge in liquid/solid and gas/solid insulation systems that are often used in power equipment, such as in cables, transformers, bushings, reactors, capacitors, circuit breakers, motors, and generators. The Kerr effect method has been used to measure the electric field distribution in liquids, such as in transformer mineral oils^(26–30) (Fig. 6). Material parameters such as charge mobility, permittivity, and resistivity can be obtained from the combination of measurement results and those of model simulation. The precise design of an insulation system is thus possible.

Surface discharge is one of the possible causes of failure of power equipment. Such a discharge is visible under some experimental conditions (Fig. 7).

By the electrooptic Pockels effect method, two-dimensional surface charge patterns on film materials can be measured. In Fig. 8, the two-dimensional surface discharge patterns on insulating materials of cellulose paper (60 μm in thickness) and Nomex T410 aramid paper (80 μm in thickness) were measured in air.⁽⁵⁴⁾ The needle/plane electrode geometry was used. The HV electrode was a steel needle with a tip radius of 40 μm . The measurements were made using triangular wave voltages of ± 5 kV with a rise time of 10 μs and a fall time of 10 ms. Both positive and negative surface charges were clearly observed [Figs. 8(b)–8(e)]. The positive surface charge patterns were branchlike, while the negative surface charge patterns were round and homogeneous. The surface charge pattern at positive polarity was larger than that at negative polarity for both the cellulose paper and the Nomex paper. However, the surface charge pattern size difference between the two types of paper was not so large at the same polarity.

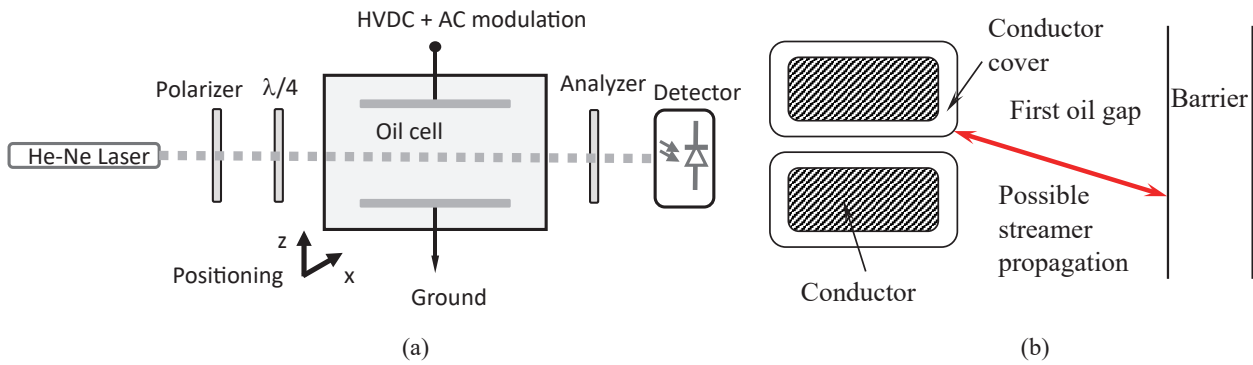


Fig. 6. (Color online) Electrooptic Kerr measurement system: (a) principle⁽²⁶⁾ and (b) sketch of a detail of transformer insulation (potential application of the Kerr method).

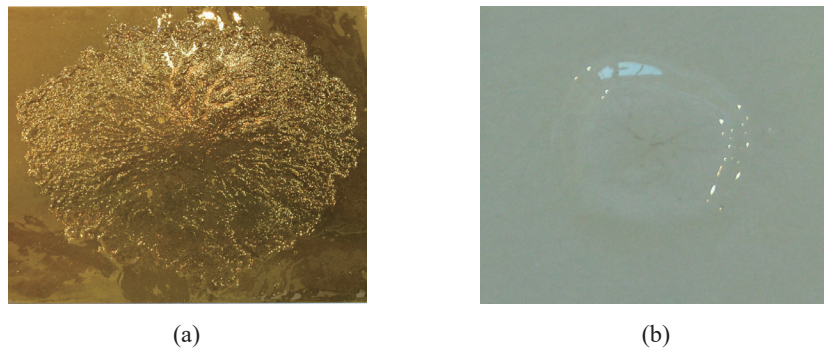


Fig. 7. (Color online) Discharge patterns under a lightning impulse voltage on an (a) oil-impregnated laminated cellulose paper surface and (b) oil-impregnated laminated Nomex T410 paper surface.

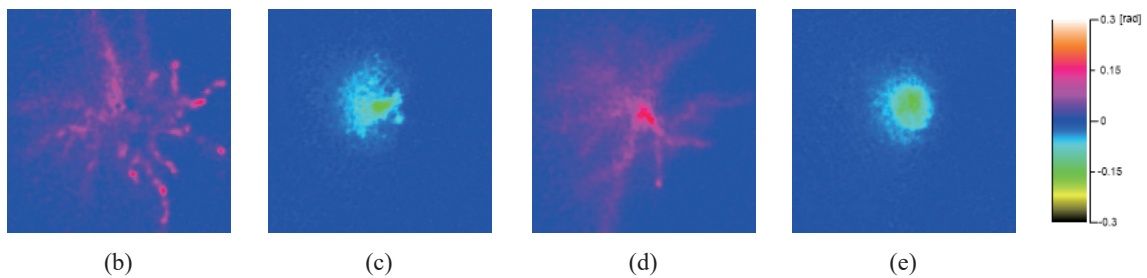
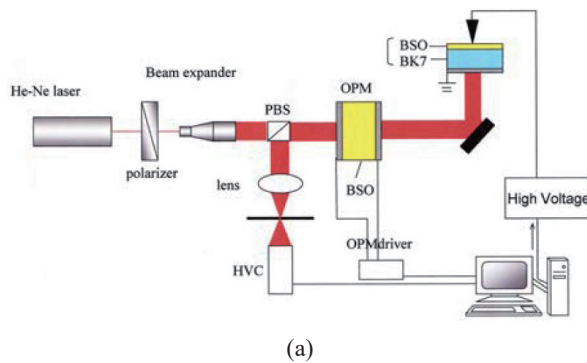


Fig. 8. (Color online) Electrooptic Pockels effect measurement system and results: (a) principle, (b) and (c) measured two-dimensional surface charge patterns on the surface of cellulose paper (60 μm in thickness) under triangular wave voltages of ± 5 kV (picture dimensions: $80 \times 80 \text{ mm}^2$), and (d) and (e) measured patterns on Nomex T410 paper (80 μm in thickness).⁽⁵⁴⁾ (b) +5 kV, cellulose paper, (c) -5 kV, cellulose paper, (d) +5 kV, Nomex paper, and (e) -5 kV, Nomex paper.

4. Conclusions

Technologies are available today to fabricate sensors on the basis of the electron beam method, the thermal pulse method, the pressure wave method, the pulsed electroacoustic wave method, the electrooptic Kerr effect, and the electrooptic Pockels effect. These sensors make it possible to measure the distribution of space charge in dielectrics and electrical insulation materials and systems quantitatively. The electron beam method is a destructive method with high resolution. All the other methods mentioned are, however, nondestructive. PWP/PEA methods are more suitable for obtaining the distribution of space charge in dielectric solids. The electrooptic Kerr method is more suitable for the measurement of two-dimensional electric fields in dielectric liquids and the Pockels effect method is more suitable for the measurement of two-dimensional surface charges on solid dielectric films. By combining measurement results with those of model simulation, the quantitative analysis and design of an insulation system for power equipment are possible.

References

- 1 T. Takada and T. Sakai: IEEE Trans. Electr. Insul. EI-18 (1983) 619.
- 2 T. Takada, T. Maeno, and H. Kushibe: Proc. 5th Int. Symp. Electrets (IEEE, 1985) p. 450.
- 3 T. Maeno, T. Futami, H. Kushibe, T. Takada, and C. M. Cooke: IEEE Trans. Electr. Insul. 23 (1988) 433.
- 4 T. Maeno, H. Kushibe, T. Takada, and C. M. Cooke: Annual Report: Conf. Electrical Insulation and Dielectric Phenomena (CEIDP) (IEEE, 1985) p. 389.
- 5 C. M. Cooke, K. A. Wright, T. Maeno, H. Kushibe, and T. Takada: Conf. Electrical Insulation and Dielectric Phenomena (CEIDP) (IEEE, 1986) p. 444.
- 6 R. S. Liu: Ph.D. Thesis, Xi'an Jiaotong University, China, 1988 (in Chinese).
- 7 P. Laurenceau, G. Dreyfus, and J. Lewiner: Phys. Rev. Lett. 38 (1977) 46.
- 8 A. Migliori and J. D. Thompson: J. Appl. Phys. 51 (1980) 479.
- 9 G. M. Sessler, J. E. West, and G. Gerhard: Phys. Rev. Lett. 48 (1982) 563.
- 10 F. Chapeau, C. Alquie, J. Lewiner, H. Auclair, Y. Pelet, and R. Jocteur: IEEE Trans. Electr. Insul. EI-21 (1986) 405.
- 11 D. K. Das-Gupta and S. B. Long: Int. Conf. Properties and Applications of Dielectric Materials (ICPADM) (IEEE, 1985) p. 403.
- 12 Y. W. Zhang, J. Li, Z. Peng, X. Qin, and Z. Xia: IEEE Electr. Insul. Mag. 17 (2001) 25.
- 13 T. Takada, J. Holboell, A. Toureille, J. Densley, N. Hampton, J. Castellon, R. Hegerberg, M. Henriksen, G. C. Montanari, M. Nagao, and P. Morshuis: Electra 223 (2005) 53.
- 14 T. Takada, J. Holboell, A. Toureille, J. Densley, N. Hampton, J. Castellon, R. Hegerberg, M. Henriksen, G. C. Montanari, M. Nagao, and P. Morshuis: Technical Brochure 288, CIGRE Task Force D1.12.01, 2006.
- 15 G. M. Sessler, J. E. West, and D. A. Berkley: Phys. Rev. Lett. 38 (1977) 368.
- 16 G. M. Sessler, J. E. West, and H. Von Seggern: J. Appl. Phys. 53 (1982) 4320.
- 17 D. W. Tong: IEEE Trans. Electr. Insul. EI-17 (1982) 377.
- 18 R. E. Collins: Appl. Phys. Lett. 26 (1975) 675.
- 19 A. S. DeReggi, C. M. Guttman, F. I. Mopsik, G. T. Davis, and M. G. Broadhurst: Phys. Rev. Lett. 40 (1978) 413.
- 20 H. Von Seggern: Appl. Phys. Lett. 33 (1978) 134.
- 21 R. S. Liu, C. Törnkvist, and U. Gäfvert: Int. Conf. Properties and Applications of Dielectric Materials (ICPADM) (IEEE, 1994) p. 139.
- 22 R. S. Liu, C. Törnkvist, and K. Johansson: Conf. Electrical Insulation and Dielectric Phenomena (CEIDP) (IEEE, 1994) p. 316.
- 23 R. S. Liu and G. Wahlström: Int. Symp. Electrical Insulation (ISEI) (IEEE, 1994) p. 103.
- 24 R. S. Liu, A. Jaksts, C. Törnkvist, and M. Bergkvist: Int. Conf. Solid Dielectrics (ICSD) (IEEE, 1998) p. 17.
- 25 M. Jeroense: Ph.D. Thesis, Delft University of Technology, 1997.

- 26 U. Gäfvert, A. Jaksts, C. Törnkvist, and L. Walfridsson: IEEE Trans. Electr. Insul. **27** (1992) 647.
- 27 M. Zahn: IEEE Trans. Dielectr. Electr. Insul. **5** (1998) 627.
- 28 T. Takada: IEEE Trans. Dielectr. Electr. Insul. **6** (1999) 519.
- 29 R. S. Liu, A. Satoh, T. Kawasaki, K. Tanaka, and T. Takada: IEEE Trans. Electr. Insul. **27** (1992) 245.
- 30 Z. R. Peng, R. S. Liu, and D. M. Tu: Int. Conf. Properties and Applications of Dielectric Materials (ICPADM) (IEEE, 1991) p. 276.
- 31 T. Kawasaki: Ph.D. Thesis, Musashi Institute of Technology in Japan, 1993.
- 32 Y. C. Zhu: Ph.D. Thesis, Musashi Institute of Technology in Japan, 1997.
- 33 T. Kawasaki, T. Terashima, Y. G. Zhu, T. Takada, and T. Maeno: J. Phys. D: Appl. Phys. **27** (1994) 1646.
- 34 P. A. Thiessen, A. Winkel, and K. Hermann: Phys. Z. **37** (1936) 511.
- 35 R. S. Liu, D. M. Tu, and Z. Y. Liu: Int. Conf. Properties and Applications of Dielectric Materials (ICPADM) (IEEE, 1988) p. 375.
- 36 J. Kerr: Phil. Mag. **50** (1875) 337.
- 37 T. Ditchi, C. Alquie, J. Lewiner, E. Favrie, and R. Jocteur: IEEE Trans. Electr. Insul. **24** (1989) 403.
- 38 S. Mahdavi, C. Alquie, and J. Lewiner: Conf. Electrical Insulation and Dielectric Phenomena (CEIDP) (IEEE, 1989) p. 296.
- 39 S. Mahdavi, C. Alquie, and J. Lewiner: Jicable 91: Proc. Intern. Conf. Polymer Insulated Power Cable (1991) p. 534.
- 40 M. Yasuda, M. Ito, and T. Takada: Jpn. J. Appl. Phys. **30** (1991) 71.
- 41 K. Fukunaga, H. Miyata, M. Sugimori, and T. Takada: Trans. Instr. Electr. Eng. Jpn., A **110** (1990) 647 (in Japanese).
- 42 N. Hozumi, T. Okamoto, and T. Imajo: Int. Symp. Electrical Insulation (ISEI) (IEEE, 1992) p. 294.
- 43 R. S. Liu, T. Takada, and N. Takasu: J. Phys. D: Appl. Phys. **26** (1993) 986.
- 44 K. Nagashima, X. Qin, Y. Tanaka, and T. Takada: Int. Conf. Solid Dielectrics (ICSD) (IEEE, 1998) p. 60.
- 45 T. Muronaka, Y. Tanaka, and T. Takada: Conf. Electrical Insulation and Dielectric Phenomena (CEIDP) (IEEE, 1996) p. 266.
- 46 M. Fu, G. Chen, A. E. Davies, Y. Tanaka, and T. Takada: Int. Conf. Properties and Applications of Dielectric Materials (ICPADM) (IEEE, 2000) p. 104.
- 47 M. Fu and G. Chen: IEE Proc. Sci. Meas. Technol. **150** (2003) 89.
- 48 N. Hozumi, T. Takeda, H. Suzuki, K. Fujii, K. Terashima, M. Hara, Y. Murata, K. Watanabe, and M. Yoshida: Electr. Eng. Jpn. **124** (1998) 16.
- 49 R. S. Liu, M. Bergkvist, and M. Jeroense: Int. Conf. Solid Dielectrics (ICSD) (IEEE, 2007) p. 438.
- 50 R. S. Liu: IEEE Electr. Insul. Mag. **29** (2013) 37.
- 51 IEC Technical Specification: IEC/TS 62758, 2012.
- 52 R. S. Liu, M. S. Wang, and D. M. Tu: Conf. Electrical Insulation and Dielectric Phenomena (CEIDP) (IEEE, 1991) p. 126.
- 53 K. Matsui, A. Miyawaki, Y. Tanaka, T. Takada, R. Liu, and T. Maeno: Proc. Int. Symp. Electr. Insul. Mater. (IEEE, 2005) p. 103.
- 54 T. Takada and R. S. Liu: Results of Collaboration between ABB and Musashi Institute of Technology (2005).